

# Detailed Studies on Turbulent Premixed Lean Flames Using Combined 1D-Raman and OH-LIF

A.Goldman\*, S.Marathe, R.Schießl, U.Maas

Institut für Technische Thermodynamik (ITT), Karlsruhe Institut für Technologie (KIT), D-76128 Karlsruhe

## Abstract

In this work, an experiment, combining 1D Raman concentration measurements of major species ( $N_2$ ,  $O_2$ ,  $CH_4$ ,  $CO_2$ ,  $H_2O$ ) and temperature with quasi-simultaneous OH radical concentration recorded using laser induced fluorescence, was conducted. The collection of the OH and Raman data (stable species and temperature) from the same probe volume makes it possible to obtain the absolute concentration values of OH using the Raman data.

Two turbulent premixed natural gas/air flames with fuel equivalence ratios of 0.68 and 0.75 are monitored. The studied flames exhibit globally stable operation in the partially extinguishing regime.

The results from the studied flames are recorded in a form of OH maps and joint PDFs of experimentally obtained scalars at several heights above the burner surface, representing different reactants/burned gases ratios.

## Introduction

In many technical applications, turbulent premixed or partially premixed combustion under lean conditions is a desired operation mode, e.g., in gasoline engines, HCCI/CAI engines or in gas turbines. Under lean conditions, chemical reactions are slower than in stoichiometric combustion, and effects associated with extinction and highly unsteady combustion phenomena can therefore become important. This makes these systems attractive candidates for studying effects that are not captured well by established combustion models [1]. For the development of improved combustion models that also cover the regime of extinction, empirical information about lean, premixed flames is still needed. Several experimental studies on turbulent non-premixed combustion have been performed using combined Raman and OH-laser induced fluorescence techniques, [2-5]. However, detailed experimental investigations on premixed flames only recently seen increased interest, especially, in context with partially premixed combustion and stratified combustion [6].

Multiscalar measurements in turbulent flames are an important key to a detailed understanding of turbulence–chemistry interaction. Combination of OH-LIF and Raman spectroscopy is a valuable diagnostic tool for this purpose.

Spontaneous Raman scattering does not require tunable excitation radiation, and the spectrum of Raman scattered light contains characteristic signatures of different molecules in the probe volume. The scattering process is not disturbed by inter-molecular collisions, so signal evaluation is independent of bath conditions. These advantages are offset by small scattering cross sections, such that single-shot Raman scattering in turbulent hydrocarbon flames allows only the detection of main species based on rovibrational Raman transitions of the Stokes side.

On the other hand, LIF in a single shot scheme allows only one spectral line detection, but with sensitivity high enough to permit an accurate monitoring of the OH radical. That, in its turn, provides much sharper indicator of rapid processes in turbulent combustion, which is not necessarily evident from stable species concentration observation.

In this work, an experiment for combined measurements of concentrations of major species ( $CO_2$ ,  $O_2$ ,  $N_2$ ,  $CH_4$  and  $H_2O$ ), temperature and OH radical concentration in turbulent premixed flames is designed. The combustor allows flame operation in a wide range of equivalence ratios and turbulence intensities. In this paper, results of two lean ( $\Phi = 0.75$  and  $\Phi = 0.68$ ) piloted jet flames, fired with a natural gas air mixture, are shown. The flames in study present stable operation in the partially extinguishing regime.

## Experimental approach

The schematics of the experimental setup are shown at figure 1.

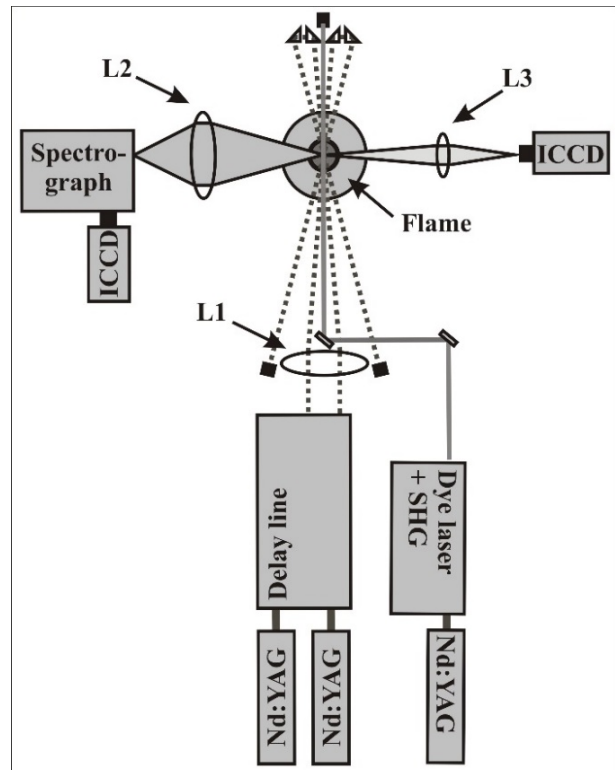


Figure 1. The experimental setup. L1 is the focusing lens for the laser beams, L2 is an achromatic collecting lens for the Raman signal and L3 is the collecting lens for the LIF signal.

\*Corresponding author: anatoly.goldman@kit.edu

### Burner configuration

The piloted jet burner (configuration presented at figure 2) has a central diameter of 30 mm. The pilot ring around the center has a slit width of 2 mm. The burner is fired with a premixture of natural gas (90 % methane) and ambient air with a total volume flow of  $\sim 55 \text{ m}^3/\text{h}$ . Flames with equivalence ratio  $\Phi = 0.75$  and  $\Phi = 0.68$  are investigated. The stoichiometric pilot flame is operated with a volume flow of  $0.66 \text{ m}^3/\text{h}$ . An air co-flow (200 mm diameter) with a flow velocity of  $\sim 0.6 \text{ m/sec}$  is used to envelope the flame. The flow field surrounding the flame is monitored using hot wire anemometer (Prosser sci. instr. AVM500). The burner is moveable along the vertical direction, to allow investigation in different heights above the burner surface.

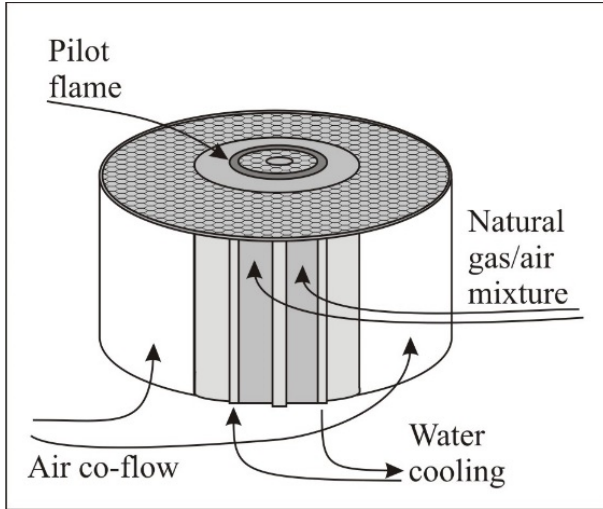


Figure 2. Premixed turbulent piloted flame burner configuration.

### Raman scattering setup

Raman scattering is excited by the radiation from two frequency-doubled Nd:YAG Lasers (B.M. industries 5022DNS10), emitting pulses (width  $\sim 5 \text{ ns}$ ) near  $532 \text{ nm}$ , with an energy of  $\sim 600 \text{ mJ}$ , and repetition rate of  $10 \text{ Hz}$ . To prevent optical breakdown in the beam focus, laser pulses are stretched using an optical delay line. The laser beams were overlapped by a cylindrical lens ( $f=250 \text{ mm}$ ) to form a nearly cylindrical focus with a diameter of  $250 \mu\text{m}$  and  $\approx 4.5 \text{ mm}$  length. The Raman signal emitted from the probe volume is collected by a spectrograph (ARC 300i) equipped with a diffraction grating ( $300/\text{mm}$ ) via an achromatic lens system (Linos Photonics, diameter  $150 \text{ mm}$ ). The spectra are recorded by an ICCD camera (PI-MAX4, Princeton Instruments). The image intensifier is activated for  $200 \text{ ns}$  at each double laser shot. The resulting spectra are divided to 25 slices along the laser beam, thus providing a special resolution of  $\approx 180 \mu\text{m}$  in the corresponding direction. The species concentrations and temperature values, derived from the recorded spectra using:

$$A_i = \frac{P \cdot x_i \cdot K_i \cdot \sigma_i(T)}{T}$$

$$\sum x_i = 1$$

where  $A_i$  is the area under a peak of specie  $i$  ( $\text{N}_2$ ,  $\text{O}_2$ ,  $\text{CH}_4$ ,  $\text{CO}_2$ ,  $\text{H}_2\text{O}$ ),  $P$  is the pressure,  $x_i$  is the molar fraction of specie  $i$ ,  $\sigma_i(T)$  is the temperature dependent Raman cross-section,  $K_i$  is a set of system related constants and  $T$  is the temperature.

Considering the sum of the five major species molar fractions as one is clearly an approximation. However, in the studied lean flame the concentrations of other species is negligible compared to the measured ones.

The area under the peaks for the calculations is chosen so, that the spectral overlap between different species signals is avoided. However, this cannot be achieved for carbon dioxide and oxygen signals. Therefore, in  $\text{CO}_2/\text{O}_2$  case, the areas were chosen in a way minimizing the overlap, followed by reduction of the overlapping area portion. These were obtained from measurements of undisturbed signals (air, McKenna flames). The overlapping areas are obviously temperature and composition dependent. Therefore, the initial guess for the concentrations of stable species and temperature is taken ignoring the overlap and the corrections are applied upon the dataset in iterative manner.

Raman cross section for each of the species was determined experimentally using the set of standard flat flames (McKenna burner) from DLR Stuttgart [7].

### OH LIF setup

The OH radical is excited using a tunable ‘‘Rhodamine special’’ (mixture of Rhodamine 6G and DCM dyes) dye laser (RadiantDye Narrowscan), pumped by the second harmonic of a Nd:YAG laser (Surelite II, Continuum). The dye laser radiation is frequency-doubled by a KDP crystal. Using spectral line at  $306.705 \text{ nm}$ , the OH radical transitions related to the  $\text{R1}(4)$  of the  $\text{A}^2\Sigma^+ \leftarrow \text{X}^2\Pi(0, 0)$  band is excited. The emitted fluorescence is collected at a right angle to the laser beam by an intensified CCD (ICCD) camera (PI-MAX3, Princeton Instruments). The ICCD intensifier is opened only for  $20 \text{ ns}$  in the beginning of a  $100 \text{ ms}$  interval between the laser pulses, thus avoiding the majority of surrounding light and the flame chemiluminescence. The molar fractions of hydroxyl radical are calculated using:

$$x_{OH} = \frac{SS_{OH} \cdot Q(T, c_i) \cdot K_B T}{F_B(T) \cdot k \sigma}$$

where  $x_{OH}$  is OH mole fraction,  $SS_{OH}$  is the strength of the collected LIF signal,  $K_B$  is the Boltzmann constant,  $F_B$  is the (temperature-dependent) Boltzmann factor for the specific rotational level used in the LIF-experiment,  $Q$  is a collisional quenching rate,  $\sigma$  is the absorption cross-section and  $K$  is a set of system related constants (collection angle, sensor efficiency etc.).

Collisional quenching calculated for each temperature/composition using data from Tamura et al. [8]

The calibration of OH-LIF signal was done using equilibrium calculation of OH concentrations in the McKenna flat flames [7].

#### Combination of LIF and Raman

The spatial correlation between Raman and LIF probe volumes is controlled by recording images of known size targets with both collection systems. The resulting uncertainty in correspondence of the Raman data to OH-LIF is dictated by the size of the image on LIF camera pixel ( $\pm 137\mu\text{m}$ ).

All lasers and acquisition systems are controlled by an ensemble of multichannel signal generators (Stanford sci. instr. DG535) allowing the collection of both Raman and LIF data within 300 ns. This allows collecting the OH and Raman data (stable species and temperature) from same probe volume and same time point, thus making it possible obtaining absolute concentrations of OH by calculating the signal quenching for each time point using the Raman data.

#### Results and Discussion

Two-dimensional OH-LIF signal maps of the flames in study are presented in figure 3. Panel a. of the figure corresponds to the leaner ( $\Phi=0.68$ ) flame and panel b. to the richer ( $\Phi=0.75$ ) flame. The use of these maps allows accurate selection of four heights above the burner (along zero radial position), which represent different combustion regimes.

Moreover, the maps show much stronger OH signal in the  $\Phi=0.75$  flame (the color/intensity scales in the two panels are identical) indicates, at least qualitatively, much higher hydroxyl radical production in the 0.75 flame.

Additionally, one can learn from the maps that the reaction zone of the 0.68 flame is located higher above the burner surface than that of the 0.75 flame (along zero radial position). That could be expected, since the cold gas velocity in the 0.68 flame is by just 0.65% smaller than in the 0.75 flame, while the laminar flame velocity is about 28% lower.

As can be seen from the OH maps, the flame possess slight asymmetry, especially visible in the  $\Phi=0.68$  flame. This caused by parasitic air flows in the combustion room. However, in the central radial position no noticeable effect on the preformed measurements is observed.

The lowest height above the burner (HAB) for subsequent Raman/OH measurements is chosen to be 6.5 cm for the 0.75 flame and 17.5 cm for the 0.68 flame. This difference is due to instability of the leaner flame in proximity to the air-cooled suction hood.

Spectra recorded at these heights consist entirely of unburned gases, with temperature only slightly elevated from the room temperature. Thus, no OH radical is detected at this height, and the chemical composition is practically identical to the supplied gases, nitrogen, oxygen, traces of water from air humidity, and methane. The region HAB = 255mm, in both flames in study, still shows, mainly, the presence of unburned gases, however

with clearly noticeable insertions of burned gases (carbon dioxide, water).

The situation changes at the third position, HAB = 325mm. The  $\Phi=0.68$  flame shows increase in amount of burned points. The majority of points is still in unburned zone. For the  $\Phi=0.75$  flame, almost equal distribution between unburned and burned (or partially burned) points is observed. Thus, clear and accurate OH concentration measurements accompany the major species concentrations for both flames.

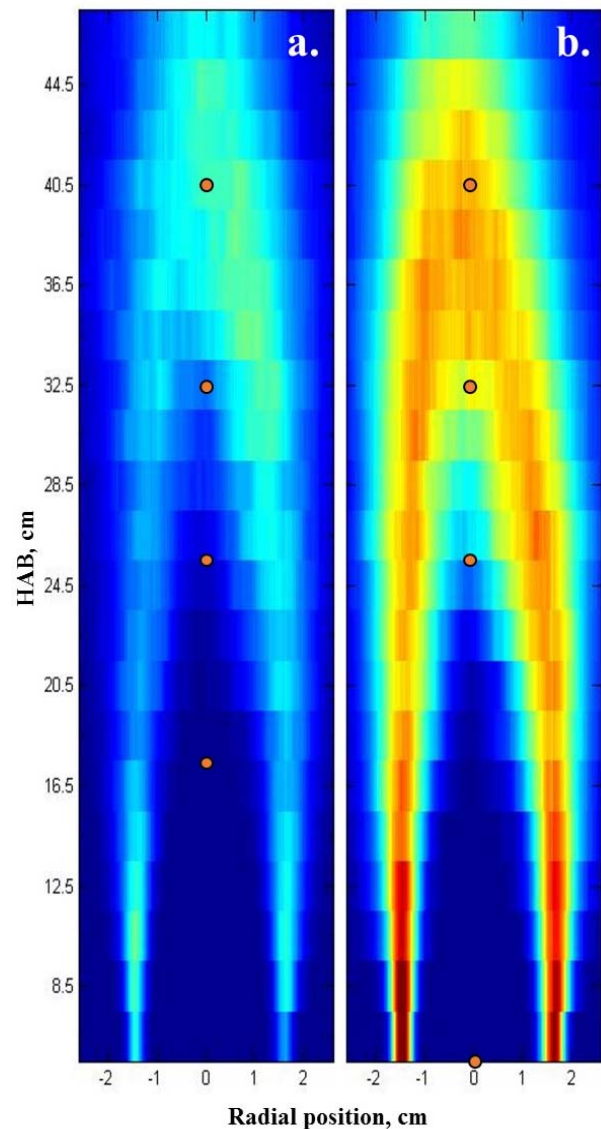


Figure 3 OH-LIF 2 dimensional maps. Panel a. is  $\Phi=0.68$  flame and panel b. is  $\Phi=0.75$  flame. The orange dots sign the target locations of the combined OH/Raman measurements.

For HAB = 405mm, the  $\Phi=0.68$  flame presents almost equal distribution between unburned and burned, much like the  $\Phi=0.75$  flame at the third height. The  $\Phi=0.75$  flame here is composed mostly of burned gases and nitrogen, however noticeable residues of methane and oxygen are clearly detectable.

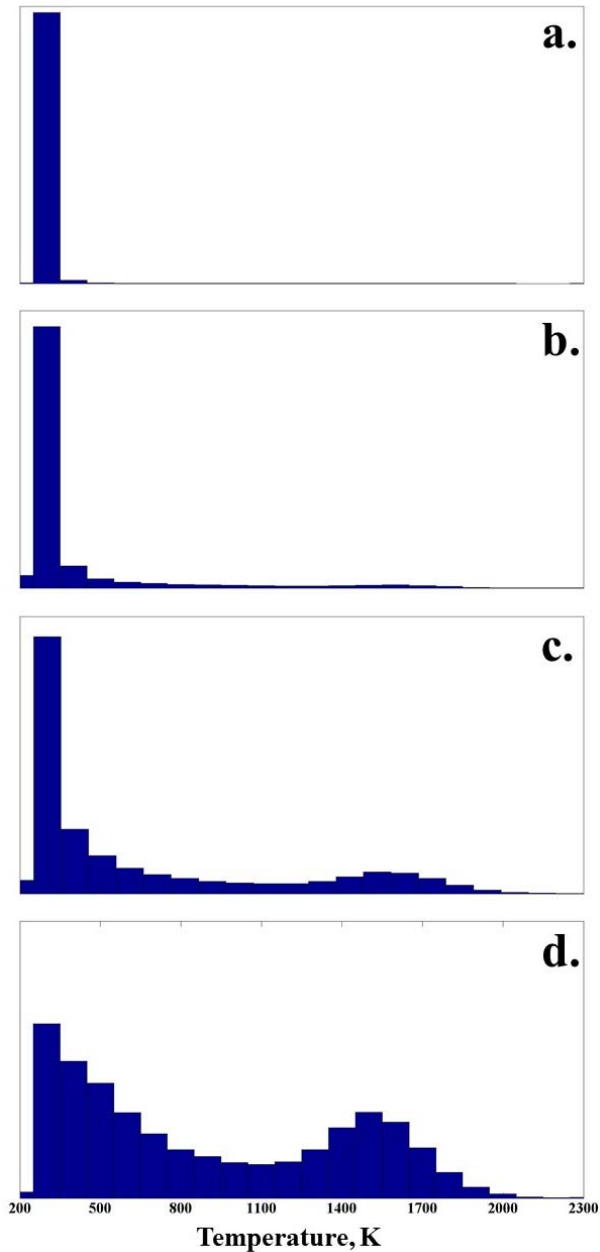


Figure 4. The  $\Phi=0.68$  flame temperature distribution. Panel a. at 17.5cm, panel b. at 25.5cm, panel c. at 32.5cm and panel d. at 40.5cm above the burner surface.

The statistical temperature distributions at each height for both the  $\Phi=0.68$  and the  $\Phi=0.75$  flames are presented on figures 4 and 5 respectively.

Comparison of temperature distributions between the  $\Phi=0.68$  flame and the  $\Phi=0.75$  flame (at third and fourth heights) shows a distinguishably lower most probable temperature of the burned gases at the  $\Phi=0.68$  flame, about 1500 K versus about 1700 K for the  $\Phi=0.75$  flame. The most probable temperatures are lower than the expected equilibrium ones ( $\sim 1800\text{K}$  and  $\sim 1900\text{K}$  respectively). However, the maximum observed temperatures are somewhat higher. That, partially, can be attributed to increased uncertainty in temperature determination at high temperatures.

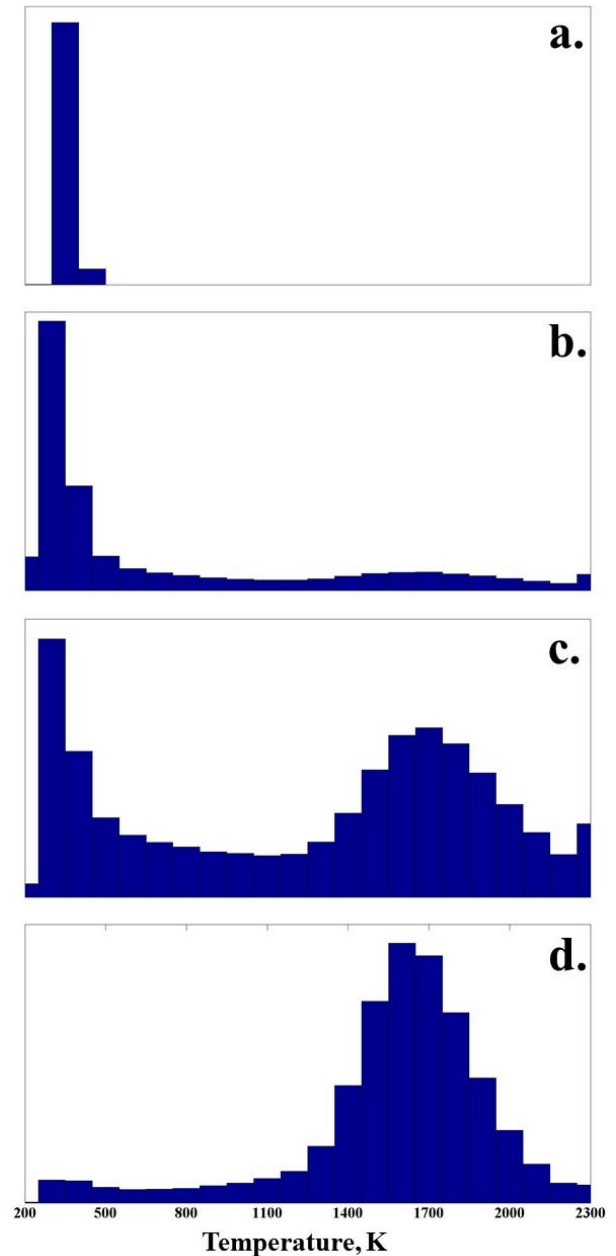


Figure 4. The  $\Phi=0.75$  flame temperature distribution. Panel a. at 6.5cm, panel b. at 25.5cm, panel c. at 32.5cm and panel d. at 40.5cm above the burner surface.

Additionally, it is important to note that in the  $\Phi=0.68$  flame, even at the fourth height (40.5 cm above the burner surface), the probability to measure unburned gas mixture temperature is noticeably higher than the probability for burned gases. This phenomenon serves as an indication of more effective local extinction in the  $\Phi=0.68$  flame compared to the  $\Phi=0.75$  flame. The OH-LIF results recorded in the flames in study are treated with Boltzmann factor for the specific rotational level (R1(4) of the  $A^2\Sigma^+ \leftarrow X^2\Pi(0,0)$  band) and the collisional quenching rate. These are calculated using a temperature and species concentration values acquired for each individual OH-LIF data point from the spatially and

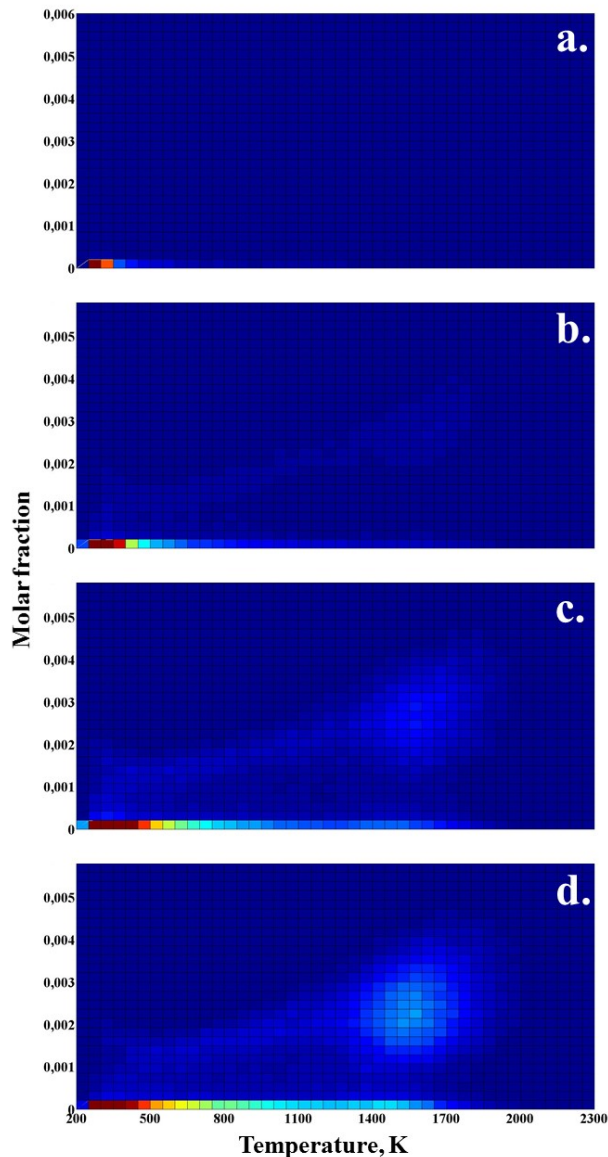


Figure 6. For the  $\Phi=0.68$  flame, the OH molar fraction/temperature JPDF. Panel a. at 17.5cm, panel b. at 25.5cm, panel c. at 32.5cm and panel d. at 40.5cm above the burner surface.

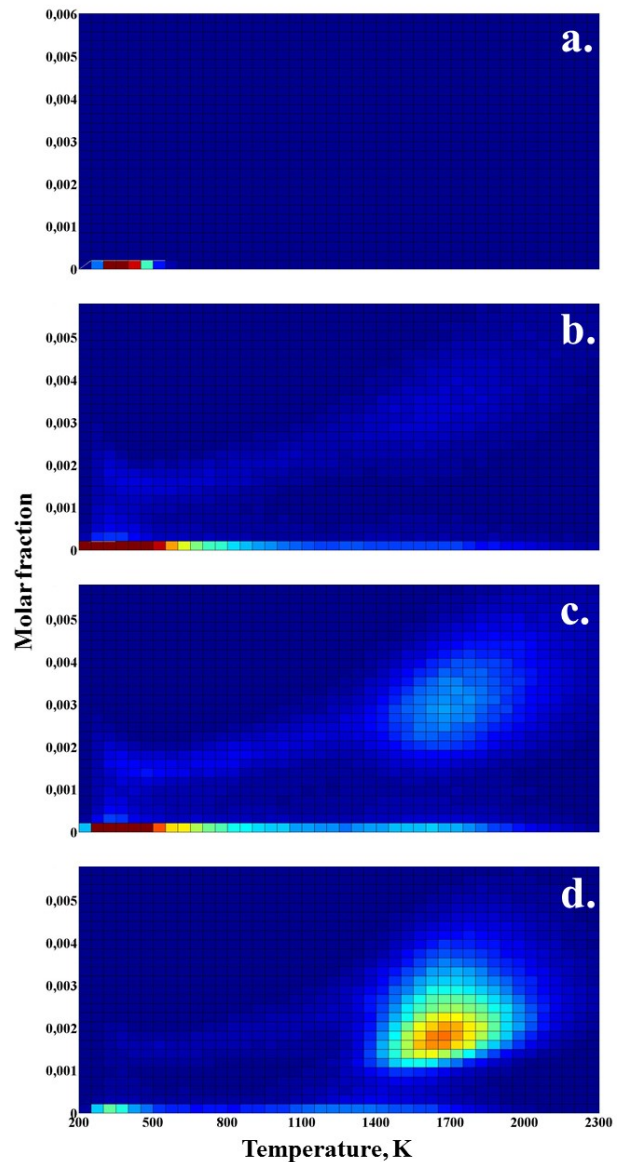


Figure 7. The  $\Phi=0.75$  flame OH molar fraction/temperature PDF. Panel a. at 6.5cm, panel b. at 25.5cm, panel c. at 32.5cm and panel d. at 40.5cm above the burner surface.

temporally corresponding Raman spectrum thus, obtaining the OH radical molar fraction.

The results are presented as two-dimensional OH molar fraction/temperature joint probability density functions (JPDF). The JPDFs for the  $\Phi=0.68$  flame are presented in figure 6, and for the  $\Phi=0.75$  in figure 7.

For both flames, the JPDFs at the lowest height visualizes the trivial result of zero OH at a temperature around 300 K. However, already at 25.5 cm a probability of finding OH molar fraction different than zero is noticeable. It is hardly traceable in the  $\Phi=0.68$  flame, but more clearly visible in the  $\Phi=0.75$  flame.

At 32.5cm above the burner surface, the OH is clearly visible in both flames. Interesting to note that, although the probability of finding OH values essentially different from zero is much higher at the  $\Phi=0.75$  flame, the mole

fraction values for a given temperature are quite similar in both flame. The fact that in the  $\Phi=0.75$  flame, higher values of OH molar fraction are present is due to the increased burned gas temperature in the fuel richer flame. At the fourth height, both flames show comparable behavior of OH molar fraction vs. temperature, alongside the much lower probability for OH being different from zero molar fraction in the  $\Phi=0.68$  flame. As in the case of temperature distributions, the joint probability density at fourth height of the  $\Phi=0.68$  flame is similar to the one at the third height of the  $\Phi=0.75$  flame, disregarding the somewhat higher temperature values at  $\Phi =0.75$

Interestingly, both flames possess “tails” of OH concentration which slowly decrease with temperature. Those “tails” are not observed in laminar flames, where OH concentration rapidly descends to zero around 1200

K. The observed tails probably can be attributed to strong turbulence and local extinction phenomena in the investigated flames.

pressure hydrocarbon flames, *Combustion and Flame*, 114:502–514 (1998)

### Conclusions

Simultaneous 1D-Raman/OH-LIF measurements were conducted in the  $\Phi=0.68$  and  $\Phi=0.75$  lean turbulent premixed natural-gas/air flames. The Raman/OH-LIF combination provides the ability for simultaneous measurements of 7 scalars (6 species and temperature), allowing a quantitative comparison of the two flames, especially with respect to increased local extinction in the leaner one.

The large data set obtained yields joint statistics of scalars, which can be used as input for statistical computational models. Further analysis will include also 1D gradient statistics, allowing more insight into the interaction of chemical reaction and transport processes.

### References

1. Geyer, D., et al., Turbulent opposed-jet flames: A critical benchmark experiment for combustion LES. *Combustion and Flame*, 2005. 143(4): p. 524-548.
2. Meier, W., et al., Raman/Rayleigh/LIF measurements in a turbulent  $\text{CH}_4/\text{H}_2/\text{N}_2$  jet diffusion flame: experimental techniques and turbulence–chemistry interaction. *Combustion and Flame*, 2000. 123(3): p. 326-343.
3. Nguyen, Q.V., et al., Raman-LIF measurements of temperature, major species, OH, and NO in a methane-air bunsen flame. *Combustion and Flame*, 1996. 105(4): p. 499-519.
4. Masri, A.R., R.W. Dibble, and R.S. Barlow, The structure of turbulent nonpremixed flames revealed by Raman-Rayleigh-LIF measurements. *Prog. Energy Combust. Sci.*, 1996. 22: p. 307-362.
5. Eckbreth, A.C., P.A. Bonczyk, and J.F. Verdieck, Combustion diagnostics by laser Raman and fluorescence techniques. *Progress in Energy and Combustion Science*, 1979. 5(4): p. 253-322.
6. Barlow, R.S., et al., Application of Raman/Rayleigh/LIF diagnostics in turbulent stratified flames. *Proc. Comb. Inst.*, 2009. 32(1): p. 945-953.
7. Prucker, S., W. Meier, and W. Stricker, A flat flame burner as calibration source for combustion research: Temperatures and species concentrations of premixed  $\text{H}_2$ /Air flames *Rev. Sci. Instrum.*, 1994. 65(9): p. 2908-2911.
8. Tamura, M, Berg, P.A., Harrington, J.E., Luque, J., Jeffries, J.B., Smith, G.P., Crosley, D.R. Collisional quenching of CH(A), OH(A), and NO(A) in low